THE TONE RANGE/TELEMETRY INTERFEROMETER TRACKING SYSTEM FOR SUPPORT OF SOUNDING ROCKET PAYLOADS

By John I. Hudgins and James R. Lease

NASA Goddard Space Flight Center

SUMMARY

The Tone Range/Telemetering (TM) Interferometer tracking system provides trajectory information for any rocket, balloon, or airborne scientific device which employs telemetry. The system was developed as a back-up and/or replacement for radar to provide the trajectory data of scientific sounding rockets.

This system is comprised of three basic systems: the Airborne, the Tone Range, and the Interferometer. The Airborne system provides ranging reception and telemetry transmission, the Tone Range system provides distance or range data, and the Interferometer system provides angular data.

The Tone Range system derives range by measuring the phase shift experienced by two tones. These tones are radiated from the ground to the Airborne system and reradiated back to the ground by the telemetry transmitter. The tones are then compared in phase with the ground standard. The phase shift of each tone is proportional to twice the slant range to the Airborne system.

The Interferometer system derives angular data by measuring the difference in electrical phase of arriving energy, radiated from the Airborne system, at two ground antennas spaced 16 wavelengths apart. Comparing the phase of the outputs of the two antennas, the azimuth of the Airborne system can be determined with respect to the antenna base line. By using four antennas, two orthogonal base lines, the azimuth and elevation angles can be derived from the electrical phase angles.

The Tone Range/TM Interferometer system has been used to track 22 sounding rockets since 1967. Several of these rockets were also tracked by radar and Radint. A comparison of the trajectories has shown that there is an average difference of 30 meters.

INTRODUCTION

The requirement for determination of the trajectory and position of spacecraft has brought about the development and deployment of many forms of tracking systems. These include tracking radars, such as the MPS-19, FPS-16, and FPQ-6 systems; multi-station Doppler systems, such as Dovap; multi-station interferometer systems, such as Minitrack;

combined Doppler interferometer systems, such as Radint; ballistic camera and theodolite installations; and recently, laser ranging systems. The principal systems used for tracking sounding rockets have been the various radars, although Radint has been used extensively in support of the grenade and pitotstatic probe experiments. Operation of the radar at NASA Wallops Station, Virginia, has been reliable without question. However, the same cannot be said of the tracking radar support at some other ranges, principally because of the lack of a sufficient number of redundant systems.

The Goddard Space Flight Center has long desired to provide some simple form of redundant tracking system to provide backup range and/or positional information. It was decided that the most advantageous and economical solution would combine the telemetry and tracking function. Two approaches were initiated: increasing the telemetry capability of the Radint tracking system, and adding a ranging capability to the standard FM/FM telemetry system. Both approaches have been successfully effected; however, the frequencies allocated to Radint have, up to now, required the use of cumbersome antennas thereby negating popular acceptance.

Several methods to obtain the desired information via standard telemetry were examined with the precision tone-range method being finally selected as the most promising. Several systems using this method had been implemented at the time of this decision. Included in these are the Sandia-AEC DME System (ref. 1) and the NASA-GRARR System (refs. 2 and 3). The techniques used in these systems were analyzed and weighed with respect to their impact on the standard telemetry processes.

A ranging frequency of 100 kHz was selected for precision ranging. Ambiguity removal frequencies of 2 kHz or 4.5 kHz were selected to support the precision ranging frequency. As with the Radint Interferometer system, the range tones are translated, with phase intact, to a frequency of 500 Hz for the ease of phase detection, digitization, and recording.

This report covers the Tone Range system and, to a lesser extent, the Telemetry Interferometer addition to the Radint system. The philosophy of the measurements is investigated, followed by system description. An analysis of data precision, accuracy and resolution is followed in the concluding section by comparisons with FPS-16 radars at Wallops Station and White Sands Missile Range.

SYMBOLS AND ABBREVIATIONS

A_{cc} coupled phase amplitude

$A_{\Delta\phi}$ range phase amplitude

c	velocity of propagation
D	distance
e_{MCV}	demodulated carrier signal
F,G,H	IRIG data channels
$FCN_I(t)$	initial sinusoidal periodic function of time
f_D	Doppler frequency
f_I	initial reference frequency
Δf	maximum carrier frequency swing incurred through modulation
J	Bessel function
M_f	a modulation constant, $2\pi \frac{\Delta f}{\omega_M}$
N	integer
R	range
$(\delta R)_{cc}$	range error as a function of cross coupling
T_I	period of f_I
t	time
t_{DG}	ground equipment delay
t_{DX}	transponder delay time
t_{FM}	time from
t_p	time accumulated between initial transmission and final reception of range tone
t_{TO}	time to
t_{XM}	transmitter delay

v	velocity
X,Y,Z	mutually orthogonal space coordinate axes
x,y,z	distance along the X,Y,Z axes
Z	altitude
θ	angle of arrival
θ_{cc}	intermodulation or cross-coupled component phase relative to $\Delta\phi$
θ_E	resulting phase error, $\tan^{-1}\frac{A_{cc}}{A_{\Delta\phi}}$
λ	wavelength
ϕ	phase
ϕ_I	initial phase
ϕ_o	accumulation of fired phases throughout the system
ϕ_R	range-tone phase
$\Delta\phi$	range-phase difference
$\omega = 2\pi f$	
ω_C	carrier frequency
$\omega_I = 2\pi f_I$	
ω_M	modulating frequency
ω_{MC}	frequency modulated carrier
ϕ_{MCI}	initial modulated carrier phase function
ϕ_{MCR}	received modulated carrier phase function

ϕ_{MCV} dynamic modulated carrier phase function

Abbreviations:

AEC	Atomic Energy Commission
AFC	automatic frequency control
AGC	automatic gain control
Az-El	azimuth-elevation
BCD	binary coded decimal
DME	distance measuring equipment
Dovap	Doppler, velocity and position
GM	Goddard meteorological
GRARR	Goddard range and range-rate system
IF	intermediate frequency
IRIG	Inter-Range Instrumentation Group
LOS	loss of signal
NASA	National Aeronautics and Space Administration
PCM-FM	pulse-coded modulation-frequency modulation
PRF	pulse repetition frequency
Radint	radio Doppler interferometer system
RF	radio frequency
UM	university meteorological

VCO voltage controlled oscillator

WWV National Bureau of Standards time radio station

PHILOSOPHY OF RANGE MEASUREMENT

The system described herein, like radar, uses the "quasi-steady state" Doppler principle (ref. 4) to obtain a range measurement. "Quasi-steady state" Doppler is a distance-propagation velocity relationship and may be thought of as an accumulation of Doppler effects, which occur during the transition from some known point to a second unknown point.

In the Tone Range system, the reference tone, a sinusoidal periodic function, $FCN_I(t) = \sin(\omega_I t + \phi_o)$, is generated and transmitted to a receiver at some fixed unknown distance R. This reference tone is retransmitted and received at the place of generation. This tone propagates over the distance 2R at the constant velocity $c = 2.997928 \times 10^5$ km/sec (the index of refraction will be assumed equal to unity for this derivation); therefore, the time accumulated between the initial transmission and final reception is $t_p = 2R/c$.

The instantaneous phase of $FCN_I(t)$ is $\phi_I = \omega_I t + \phi_o$, where ϕ_o is the accumulation of fixed phases throughout the system. These fixed phases will be assumed constant and equal to zero for the purposes of simplicity of derivation, but will be resurrected during the discussion of accuracy.

While $\phi_I = \omega_I t$, the phase of the returned tone ϕ_R, which has undergone a trip of 2R and been delayed by a period $2R/c$ is $\phi_R = \omega_I(t - 2R/c)$; this ϕ_R shall be called the range tone phase. The term, $2R/c$ is subtracted since ϕ_R is a sample of a phase generated at an earlier time than ϕ_I. In comparing these two tone phases we find ω unchanged, with the phase difference strictly contributed by the propagation time. The range R may be found from a measurement of phase difference:

$$\Delta\phi = \phi_I - \phi_R = \frac{2\omega_I R}{c}$$

$$R = \frac{c\Delta\phi}{2\omega_I}$$

Since $\omega_I = 2\pi f_I = 2\pi/T_I$, where T_I is the period of f_I, ϕ becomes ambiguous at intervals of 2π, that is, $\phi_{2\pi} \equiv \phi_o \equiv \phi_{4\pi} \equiv \phi_{N2\pi}$. On examining $\Delta\phi$ the same periodicity of ambiguity is noted. Rearranging the equation for R,

$$R = \frac{c}{2f_I} \cdot \frac{\Delta\phi}{2\pi}$$

When $\Delta\phi = N2\pi$, R assumes the same value $c/2f_I$. Between these points R is a linear function of $\Delta\phi$. A plot of $\Delta\phi$ with respect to range is shown in sketch (a).

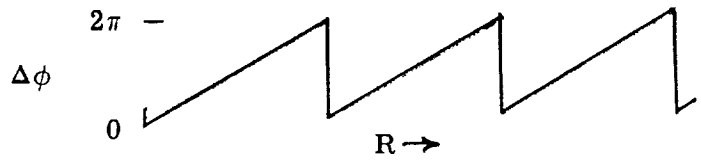

Sketch (a)

This ambiguity points out a necessity of design consideration. The maximum expected change in range may not exceed $c/2f_I$ without incurring a doubt concerning how many ambiguous cycles of $\Delta\phi$ have occurred since the last observation. The choice of a $c/2f_I$ sufficiently large to handle expected changes in range, leads generally to a more coarse measurement of $\Delta\phi$ and thus ΔR. In general, two methods of overcoming this difficulty are used, the first is constant observation and integration of ambiguities, the second is the use of more than one tone to define range. The multiple tone approach selects a high frequency tone for high range resolution plus lower frequency tones to resolve ambiguities in the higher frequency tones. The second approach is, of course, preferable since loss of data or observation time may be beyond the control of the observer.

Earlier it was mentioned that the "quasi-steady state" Doppler was an accumulation of Doppler motion effects, that is, to obtain the observed phase shift, the observed instantaneous frequency must change during a transition in range. This is illustrated by differentiating ϕ_R with respect to time

$$\phi_R = 2\pi f_I\left(t - \frac{2R}{c}\right)$$

and

$$\frac{d\phi_R}{dt} = 2\pi f_I\left(1 - \frac{2}{c}\frac{dR}{dt}\right) = 2\pi f_I\left(1 - \frac{2v}{c}\right)$$

This expression is the classic nonrelativistic Doppler equation, $f_D = \frac{2v}{c} f_I$, where f_D is the Doppler frequency or observed change in frequency resulting from motion.

The ranging frequencies or tones selected for use with the Tone Ranging System were based primarily on noninterference with standard IRIG FM/FM data channels and

conformance with existing system limitations. At present the high resolution or "Fine" ranging tone is 100 kHz (1.5 km) with one ambiguity resolving "Coarse" tone at one of two frequencies 2 kHz (75 km) and 4.5 kHz $\left(33\frac{1}{3}\text{ km}\right)$. Since neither of these "Coarse," or ambiguity removal, tones gives unambiguous range in excess of the expected, deductive logic plus some knowledge of trajectories is required to find the exact range.

Obviously, the frequencies selected are of too long a wavelength to be transmitted directly and instead modulate a carrier frequency. Questions naturally arise with regard to the impact of this "piggyback" mode of transportation on the measurement of interest.

A frequency modulated carrier may be expressed in the following fashion:

$$\omega_{MC} = \omega_C + 2\pi\Delta f \cos \omega_M t$$

where

ω_C the carrier frequency

ω_M the modulating frequency

ω the instantaneous angular velocity or frequency

Δf the maximum carrier frequency swing incurred through modulation

M_f a modulation constant, $2\pi \frac{\Delta f}{\omega_M}$

By integrating we obtain the modulated carrier phase function of time

$$\phi_{MCI} = \omega_C t + 2\pi \frac{\Delta f}{\omega_M} \sin \omega_M t = \omega_C t + M_f \sin \omega_M t$$

The steady-state carrier phase after undergoing the transit to and from a point at range R is

$$\phi_{MCR} = \omega_C\left(t - \frac{2R}{c}\right) + M_f \sin \omega_M\left(t - \frac{2R}{c}\right)$$

The instantaneous dynamic frequency of ϕ_{MCR} is obtained by differentiating ϕ_{MCR} with respect to time

$$\frac{d\phi_{MCR}}{dt} = \omega_C\left(1 - \frac{2v}{c}\right) - M_f\left[\cos \omega_M\left(t - \frac{2R}{c}\right)\right]\left(1 - \frac{2v}{c}\right) = \left(1 - \frac{2v}{c}\right)\left[\omega_C - M_f \cos \omega_M\left(t - \frac{2R}{c}\right)\right]$$

The returned phase for the case of motion ϕ_{MCV} is derived by integrating the above equation

$$\phi_{MCV} = \int_t d\phi_{MCR} = \left(1 - 2\frac{v}{c}\right)\left[\omega_C t - M_f \sin \omega_M\left(t - \frac{2R}{c}\right)\right]$$

The carrier may then be expressed as

$$e_{MCV} = \sin\left\{\left(1 - \frac{2v}{c}\right)\left[\omega_C t - M_f \sin \omega_M\left(t - \frac{2R}{c}\right)\right]\right\}$$

This can be written in the form

$$e_{MCV} = \sin \omega_C t\left(1 - \frac{2v}{c}\right)\cos\left[M_f\left(1 - 2\frac{v}{c}\right)\sin \omega_M\left(t - 2\frac{R}{c}\right)\right]$$
$$+ \cos \omega_C t\left(1 - 2\frac{v}{c}\right)\sin\left[M_f\left(1 - 2\frac{v}{c}\right)\sin \omega_M\left(t - 2\frac{R}{c}\right)\right]$$

This may be manipulated further since $\cos\left[M_f\left(1 - 2\frac{v}{c}\right)\sin \omega_M\left(t - 2\frac{R}{c}\right)\right]$ expanded can be expressed as a Bessel function of argument $M_f\left(1 - 2\frac{v}{c}\right)$, which is written

$$J_0\left[M_f\left(1 - 2\frac{v}{c}\right)\right] + 2J_2\left[M_f\left(1 - 2\frac{v}{c}\right)\cos 2\omega_M\left(t - 2\frac{R}{c}\right) + \ldots\right]$$

Similar expansion of $\sin\left[M_f\left(1 - 2\frac{v}{c}\right)\sin \omega_M\left(t - 2\frac{R}{c}\right)\right]$ yields

$$2J_1\left[M_f\left(1 - 2\frac{v}{c}\right)\sin \omega_M\left(t - 2\frac{R}{c}\right) + 2J_3\left[M_f\left(1 - 2\frac{v}{c}\right)\right]\sin 3\omega_M\left(t - 2\frac{R}{c}\right) + \ldots\right]$$

Reinstating these Bessel functions in the equation for e_{MCV}, using only the first order terms for simplicity of expression, yields

$$e_{MCV} = J_0\left[M_f\left(1 - 2\frac{v}{c}\right)\right]\sin \omega_C t\left(1 - 2\frac{v}{c}\right) + J_1\left[M_f\left(1 - 2\frac{v}{c}\right)A\right]$$

where $A = 2 \sin \omega_M\left(t - 2\frac{R}{c}\right)\cos \omega_C t\left(1 - 2\frac{v}{c}\right)$. Expanding A, it is rewritten in the form

$$e_{MCV} = J_0\left[M_f\left(1 - 2\frac{v}{c}\right)\right]\sin \omega_C t\left(1 - 2\frac{v}{c}\right) + J_1\left[M_f\left(1 - 2\frac{v}{c}\right)\right]\left\{\underbrace{\sin\left[\omega_C t\left(1 - 2\frac{v}{c}\right) + \omega_M\left(t - 2\frac{R}{c}\right)\right]}_{\text{1st upper sideband}} - \underbrace{\sin\left[\omega_C t\left(1 - 2\frac{v}{c}\right) - \omega_M\left(t - 2\frac{R}{c}\right)\right]}_{\text{1st lower sideband}}\right\}$$

The simplest expression for demodulation is translation to zero frequency thus:

$$e_{MCV} = J_1\left[M_f\left(1 - 2\frac{v}{c}\right)\right]\sin \omega_M\left(t - 2\frac{R}{c}\right)$$

The phase $\omega_M\left(t - 2\frac{R}{c}\right)$ is therefore recovered intact!

Any periodic ranging system, such as pulsed radar, operates by the principles outlined above. The principal difference between tone ranging and radar is the trade-off between power and bandwidth. In radar the PRF is the ambiguity removing frequency, with the frequency of the uppermost usable Fourier component of the pulse forming the precision ranging frequency. Due to the wide bandwidth required to accommodate a radar video spectrum and the commensurate noise introduced in this wide bandwidth, signal levels must be high to obtain reasonable signal to noise. Added to this, is the poor "transponder" formed by the almost isotropic reflection from a small object thus forming further demand for high radiated power density to obtain reasonable signal levels at the receiver. To obtain these high power densities and signal levels, the peak power output must be as high as possible, plus antenna gain must be maximized. To obtain the latter, beamwidth is narrowed as much as possible, thus presenting a problem of acquisition. The Tone Range/TM Interferometer system uses hemispheric antenna coverage where feasible, and beamwidths on the order of 60^o where some gain is desired. Relative ease of acquisition of Radar and Tone Range/TM Interferometer can be compared with using a searchlight to follow a bird at night versus following a bird in broad daylight with your eyes. In addition, since Tone Ranging and the TM Interferometer systems are both narrow band systems (<10-Hz bandwidth can accommodate the signals) a very favorable signal to noise relationship exists.

PHILOSOPHY OF ANGLE MEASUREMENT

This section of the report will not go into detailed description and analysis of the Interferometer since much of this can be found in reference 5. This reference provides

a detailed description and some accuracy considerations of the Radint system.

The Interferometer system is the radio frequency analog of Fraunhoffer optical interference phenomena. Figure 1 depicts one axis of the interferometer shown at the moment of arrival of a plane wave front at the east antenna. In the time period taken for the wave to arrive at the west antenna, the phase at the east antenna will have changed. If the antennas are spaced exactly 1 wavelength apart, the electrical phase difference of the signals received simultaneously at the two antennas is representative of the cosine of the space angle of arrival of the wave front with respect to the plane of the Interferometer. As the antenna spacing is opened up to 2 wavelengths, ambiguities begin to appear since the same electrical phase, 0^{o}, is present for wave arrivals from the east and west horizons as well as that arriving parallel to the Interferometer axis. Although ambiguous, the electrical phase angle in degrees now represents half the space angle. As the axis increases in numbers of wavelength, ambiguities increase; however, the precision of measurement also increases proportionally. Each ambiguity is termed a "lobe." There are 32 such lobes in a 16-wavelength interferometer. Figure 2 is an attempt to indicate the three-dimensional configuration of the lobe pattern for half the Interferometer pattern. Depicted in this illustration is what might be termed a "core sample" of the lobe pattern. The lobes realistically extend to infinity. Two mutually normal Interferometer axes are used; their combined output defines a vector which includes the center of the Interferometer array, the object being tracked, and results from the intersection of two conical surfaces of constant phase, one associated with each Interferometer. Removing ambiguities by using close-spaced antennas is not at present deemed necessary, since integrated tracking from launch to end of flight or LOS has proven effective and reliable for over 300 Radint operations. However, where ambiguity removal is required, for example, signal not available at launch, this may be accomplished by the addition of one antenna and associated electronics for each axis.

The relationship between measured phase and the space angle of arrival is derived herein. In sketch (b), an equiphase wavefront is shown at the moment it impinges the

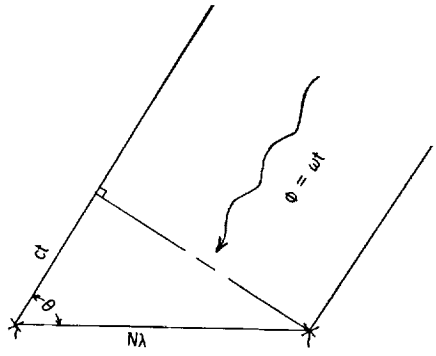

Sketch (b)

right antenna of an interferometer. The phase distribution in the direction of propagation is $\phi = 2\pi ft$ where ct is the distance the wavefront must travel to reach the left antenna and f is frequency of the arriving energy. The Interferometer base is depicted as having a length of $N\lambda$. Geometrically, the desired information, $\cos \theta = \frac{ct}{N\lambda}$. Restating ϕ in terms of λ, $\phi = \frac{2\pi ct}{\lambda} \frac{N}{N}$, and rearranging yields

$$\phi = 2\pi N \frac{ct}{N\lambda} = 2\pi N \cos \theta$$

therefore $\cos \theta = \frac{\phi}{2\pi N}$.

SYSTEM DESCRIPTION

Tone Range System

The Tone Range system is comprised of several subsystems. These are

Telemetry receiver, antenna, and preamplifier
Precision tone generator and synthesizer
Tone reference transmitter and antenna
Tone translator
Analog phase comparator and recorder
Servo phase comparator and grey code to BCD converter
Airborne receiver and telemetry transmitter

A simplified block diagram of the Tone Range/TM Interferometer system is shown in figure 3. The heart of this system is the precision tone generator. This is normally a Hewlett-Packard HP 5245L counter from which a 1-MHz output is used to synthesize the required frequencies. (Other counter functions include driving the timing and digital systems.)

In the tone frequency synthesizer, the 1-MHz input is applied to divider chains to produce several phase coherent frequencies. The divider chains are commonly reset at a 250-Hz rate to insure against lock-up and undesired noise switching. In the second Tone system, this unit provides

Frequency	To	Purpose
100 kHz	Reference transmitter	Uplink modulation
104.5 kHz	Reference transmitter	Uplink modulation
500 Hz	Reference to analog phase detectors and servo phase detectors	Comparison with range tones

Frequency	To	Purpose
160 kHz	Tone translator	Conversion of 100 kHz range tone to 160 kHz
25 kHz	Tone translator	Conversion of 60 kHz to 35 kHz
31.25 kHz	Tone translator	Conversion of 35 kHz to 3.75 kHz
4.25 kHz	Tone translator	Conversion of 3.75 kHz to 500 kHz + ϕ
3.4 kHz	Tone translator	Conversion of 4.5 kHz range tone to 1.1 kHz
1.6 kHz	Tone translator	Conversion of 1.1 kHz to 500 Hz + ϕ

The tone translator accepts the received mixed video and extracts the 100-kHz and 104.5-kHz range tones from the telemetry data via a 102.5-kHz, 6-percent bandwidth filter. These multiplexed range tones, dc referenced to signal common at the filter output, are applied to a diode limiter. This serves to establish a fixed signal level, as well as to establish the nonlinear function for separation of the coarse 4.5-kHz range tone. The limiter output is applied through buffer amplifiers to a 100-kHz, 2-percent bandwidth filter and a 4.5-kHz, 6-percent bandwidth filter for separation of the Fine and Coarse range tones. The 100-kHz and 4.5-kHz tones are mixed with the phase-coherent translating frequencies as indicated in the above table.

The analog phase detectors generate asymmetrical square waves, the degree of asymmetry of which is linearly proportional to the phase difference $\Delta\phi$ between the 500-Hz reference and 500-Hz + ϕ range tones. This square wave is integrated to form an output voltage linearly proportional to $\Delta\phi$.

The outputs of the analog phase detectors are presented versus time by a Brush MK 280 Analog Recorder. Figure 4 depicts a typical range analog record.

The 500-kHz reference and range tones are also applied to the servo phase detector. Here these two signals are compared in phase by a synchroresolver, the output of which is a voltage proportional to the phase difference. This resolver is coupled by a gear train to a motor, the control of which is derived from the resolver output. Feedback is obtained in this manner and maintains, through mechanical rotation, zero phase difference between reference and range tone resolver windings.

The feedback loop bandwidth is selectable at 0.1, 1, and 10 Hz, thus allowing variable control over dynamic and signal-to-noise characteristics.

The resolver-motor gear train provides other shaft outputs. With their output rotations referenced to the resolver, these are

1-km analog potential output	2:3
500-km analog potential output	1:300
digital encoder	1:600

The potentiometer outputs of the range servo phase detector are not commonly used, however, the 500-km range potential will provide position data for an X, Y, and Z position analog computer now being designed.

The Datex Shaft Encoder provides a special normalized Datex code. Conversion of this code to 8, 4, 2, 1 BCD code is also performed by the servo unit. This is in a form easily processed by the Radint digital system.

In the airborne portion of the system, the only special equipment required is the tone receiver and its associated antenna. The received signal, generally 550 MHz, is demodulated and the resultant range tone signals are multiplexed with the data VCO outputs. The range tone signals are not preemphasized in accordance with their frequency relationship to the VCO frequencies. They are generally accorded 15 to 20 percent of the total telemetry transmitter deviation or ±15 kHz, whichever is less. This is done to limit the effect of tracking on data acquisition, that is, placing the priority on the acquisition of experimental data. Figures 5 and 6 show the airborne components necessary for tone ranging.

Support Subsystems

In addition to the subsystems specific to the Tone Range system, there are several of the Radint support subsystems which are often used in support of the Tone Range/TM Interferometer system. These are

Tape record-playback system
Timing system
Digital system
Data link system
Station multiplex
NASA 28 bit international timing system

Tape record-playback system.- This system, selected for low skew characteristics, provides a permanent record of Tone and Interferometer reference plus phase information. In addition, flight time, voice annotation, and other pertinent information is recorded via the station multiplex.

Timing system.- This system is activated by a launcher-mounted microswitch. The system counts, displays, and encodes flight time. It also provides encoded time for analog records, a visual display, and encoded time for annotation of the tape record. The timing sequence is also activated in the tape playback mode.

Digital system.- This system accepts grey coded Datex information from the Interferometer servo system, BCD time from the timing system, plus other pertinent information. It processes all data to 8, 4, 2, 1 BCD, and provides a punched paper tape containing all information pertinent to the tracking function.

Data link system.- This system accepts paper tape reader output and converts it to a tone format acceptable for transmission of digital data over commercial telephone lines.

Station multiplex.- This system uses multiplexed VCO's to combine several signals, such as receiver AGC levels, voice annotation, and other tracking function events for tape recording.

NASA 28 bit international timing system.- This system incorporates an extremely stable frequency source, from which it derives several forms of coded time for annotation of records. Time synchronization is provided via reception of WWV time signals. The coded time includes day of the year, hours, minutes, and seconds and is usually set to present Zulu time. A slow 28 bit, 2 parts per second code is used for analog record annotation.

Interferometer System

The Interferometer system consists of the antenna subsystem, the receiver subsystem, the servo phase measuring unit, and the Az-El plotter. A magnetic tape recorder and a digital system, which includes a paper tape punch, are used in the operation of both the interferometer and the Doppler portions of the station. Figure 7 depicts this system's functions in somewhat greater detail.

Antennas.- Each axis of the interferometer uses two antennas, 16 wavelengths apart; the antenna elements are spaced 1/4-wavelength above a ground plane. Each antenna is a pair of crossed dipoles, connected in circularly polarized configuration. Circularity of receiving, necessary because of the rotation of the rocket, is achieved by cutting the quarter-wave sections to a length that will cause them to be inductive, and coupling directly to two elements while connecting capacitively to the other two. Connection is made to the coaxial transmission line through a "balun" (balanced to unbalanced) transformer. It is essential for each antenna and transmission line of a pair to have the same phase characteristics. Pairs of antennas are chosen for their similarity of characteristics. Transmission lines are cut to the same integral number of wavelengths. Connections are made to the receivers through coaxial switches, so that a locally generated RF signal can be applied to the receivers for alinement purposes.

Signal processing.- Low-noise preamplifiers provide about 30-dB gain for the incoming 244.3-MHz signals from the antennas plus conversion to 73.6 MHz. The preamplifiers are followed by mixer stages. The local oscillator signal to the north and east mixers is 67.12 MHz; to the south and west mixers it is 67.1205 MHz. The 6.48- and 6.4795-MHz outputs of the north and south mixers, respectively, are combined in an adder and sent through a common IF channel; likewise, the outputs of the east and the west. A second conversion is made, giving IF's of 465 kHz for the north and east mixers and

465.5 kHz for the south and west. The detected output for each axis is 500 Hz ± phase difference between the two signals arriving at the antennas.

Phase measurement.- The phase of each of the two 500-Hz ± phase signals is compared with that of the 500-Hz reference signal by means of two different types of phase-measuring equipment: servo phasemeter tracking filter and electronic, giving an analog output.

Servo phasemeter: The servo phasemeter is an electromechanical system which converts electrical phase differences into shaft angles. These are in turn converted to direction cosines in both analog and digital form.

In this system, the 500-Hz ± phase-shift signal is fed via a motor-driven resolver phase-shifter to an analog-phase detector. Here, any phase difference between the phase-shift signal and the reference 500-Hz input results in a dc voltage. This voltage is amplified and applied to the control winding of a magnetic amplifier. The output of the magnetic amplifier, 400-Hz power level controlled by the amplifier, is applied to a servomotor, which is coupled to the resolver through a gear reduction. The action of this loop is such that the resolver is driven in a direction to bring its output into phase with the reference 500 Hz. If the phase of the incoming signal continues to change, the resolver rotates to track it. Since one rotation of the shaft gives a 360^{o} phase shift, 32 revolutions are required to track a signal source from one horizon to the other. So that unambiguous analog and digital data can be provided, a coarse potentiometer and the shaft encoder are geared down from the resolver shaft so as to give one continuous set of readings from one horizon to the other. The shaft encoder gives outputs which can be converted to decimal numbers, -.9999 to +.9999, corresponding to the direction cosines of the angles of the signals source with respect to the station. Positive and negative voltages are connected to the ends of the potentiometers so the voltage at the center of the pot is zero volts. This corresponds to a signal arriving from directly overhead (90^{o}). The shaft encoder is set to give an output of .0000 under the same conditions. Then for north or east signals, the digital output of the encoder and the voltage output of the potentiometer will be positive, while south or west directions give negative readouts. In each case, the magnitude is proportional to the cosine of the angle. However, since the servo phasemeter would lock in at any one of 32 different readings, it is necessary that the two servo systems be set to the cosines corresponding to the direction of the launch site before the feedback loop is closed.

Electronic phasemeter: An old but effective form of interferometer phase measuring technique is still in use as a redundant readout and signal loss-return code identification. Each interferometer axis 500-Hz signal is fed into an integrating-type phase detector where the signal phase is compared with that of the reference 500 Hz. Any phase difference produces an output voltage whose magnitude and polarity corresponds to the

phase difference. Each of the two analog signals drives a pen of the analog recorder. The data thus obtained are ambiguous, in that a given voltage can indicate any one of 64 different angles. It can be resolved by counting positive slope zero crossings from a known starting point and, thus, would serve as backup data in case of failure to record the other forms of data or as an aid in resolving any difficulties with the digital data.

Data presentation.- The real-time readouts of the interferometer portion of the Radint station are the Az-El plot and the pen recording of the analog data from the electronic and servo phasemeters.

Az-El plotter: An X-Y plotter is an ink recorder having an arm movable in the direction of X-axis, and a pen which moves along the arm in the direction of the Y-axis. It uses a single sheet of paper which is held stationary. The output of the analog potentiometer of the N-S servo phasemeter is applied to the Y-axis and the E-W is connected to the X-axis. A special graph paper is used which, by the geometry of line spacing, performs the conversion from directional cosines to azimuth and elevation coordinates. Because of this ability to transform the data from one set of coordinates to another, the Az-El plotter may be considered as a simple analog computer. This idea can be carried an additional step by any station which is required to furnish Range Safety data. To accomplish this, the course range analog output is processed to provide analog voltages proportional to the slant range. These voltages are used to feed the X-1 analog potentiometers. The outputs of the potentiometers are now directly portional to the X and Y components of the ground range and are used to drive one of the large X-Y plotting boards to display the rocket position in relation to range boundaries, and so on.

The Az-El plot provides an indication that a normal flight has taken place and that the equipment is functioning correctly.

Analog plot: The pen recording of the outputs of the two analog phase detectors indicate flight and equipment performance. It is also an immediately available source of very accurate angular data for on-site data reduction if necessary. Figure 8 is a replica of the continuous Interferometer analog output.

SURVEY OF SYSTEM CAPABILITIES

Tone Range

Four categories define the capabilities of any measurement system:

Accuracy – the ability of the system design to limit random statistical variations, such as noise plus the ability to define and compensate for systematic variations. Accuracy is largely tied to the system output signal to noise and calibration.

Precision – this relates to the granularity of the measuring device. In tone ranging this is governed by the highest frequency tone.

Resolution – the granularity of the system output presentation; the least significant bit in the digital output; the least definable changes in an analog output.

Ambiguity – the ability of a system to make nonambiguous measurement.

Accuracy.- A listing of system problem areas which could affect accuracy follows.

(1) System video and resonant circuit phase effects of Doppler shift and transmitter stability.
   a. Airborne receiver converter, IF, and video filter response.
   b. Airborne transmitter multiplier and output tanks.
   c. Antenna bandwidths.
   d. Ground receiver converter, IF, and video response.

(2) Lack of knowledge of system fixed phase shifts.

(3) Group delay in tone processive circuits.
   a. Those items listed in (1).
   b. Tone translator.
   c. Phase comparator analog output filter.
   d. Servo comparator loop delay.

(4) Reference tone stability. Besides providing a cumulative error with cumulative range, this could also provide additional phase errors in those areas listed in (1) and (3).

(5) Phase shift as a function of dynamic level. Affects all problem areas listed above plus the video limit circuitry.

(6) Cross coupling and intermodulation components creating false phase.

(7) Poor signal to noise at phase comparator.

Referring back to accuracy problem area (1), the following steps have been taken in system video and RF design to eliminate or minimize the problem:

1. Deviation of the Fine Range Tone (100 kHz) at the reference transmitter is limited to a $M_f < 0.5$; thus all but eliminating the 2d and higher order sidebands from contributing to the signal.

2. Airborne IF bandwidth is 500 kHz wide.

3. Ground receiver IF and video-filter bandwidths are 750 kHz and 300 kHz minimum, respectively. AFC is used to maintain center in the IF bandwidth.

The telemetry transmitters and antennas used are standard, but of sufficient bandwidth to limit measured offset frequency phase excursions to negligible amounts.

Problem area (2) concerns the time at which a measurement is recorded versus the time that the measurement was made. Figure 9 illustrates the situation covered by this analysis for a vehicle moving at a constant velocity with respect to the ground station.

Assume that at t_0, the phase ϕ_I is present at the phase comparator and the input to the reference transmitter modulation circuitry. The vehicle traverses the distance to D_1 before the signal is radiated. The time of propagation t_{TO} to point D_2 is part of the measurement that is desired. During the transponder delay time t_{DX} the rocket traverses the distance $D_3 - D_2$, following this, the time of propagation t_{FM} is the second portion of the desired measurement. During the ground processing delay t_{DG} the vehicle traverses the further distance to point D_5. This is the actual position of the rocket when the measurement is recorded with respect to time; however, the range recorded is a function of $\frac{t_{TO} + t_{FM}}{2}$ or the average time of propagation and implies the range corresponds to position D_3, but is recorded at time t_5.

The propagation time from a point $D_3 = 150$ km to ground is 500 μsec. A nominally high radial velocity for a vehicle in the post-burn phase is 1000 m/sec. The error created by propagation time for this example, would thus be 0.5 meter. This error is noncumulative but varies directly with range.

For a motionless payload, the other delays shown are essentially fixed and can be compensated for by adding an equal delay to ϕ_I. However, when the vehicle is in motion, these delays must be limited to minimize the amount of vehicle motion occurring during the measurement process. To obtain a real-time measurement error $\leq$1 meter resulting from system fixed delays for a vehicle radial velocity of 1 km/sec, the sum total of the delays must be $\leq$1 msec.

Where commercial equipment, such as the telemetry receiver and the analog recorder, is used, delays are fixed, leaving the slack to be taken care of, if possible, in the design of the transmitter modulation circuitry and tone processer.

The 100-kHz delays, measured in the various system components, are as follows:

System components	Delay for –	
	100 kHz	4.5 kHz
Up link (TRF receiver)	42 μsec	1 msec
Down link (DEI receiver)	18 μsec	10 μsec
Tone translator	3 msec	10 msec

Uncompensated differential delays between the Coarse and Fine tones can create unresolvable ambiguity in position of a vehicle, for which the fine range has not been

integrated from a known position. The wide-band video circuitry, the receivers, and the transmitter exhibit phase delays linearly proportional to frequency. The translator circuits do not exhibit this criteria. The determining phase shift is that exhibited by the Coarse translator chain with delay added to the Fine chain to regain proportionality.

The system, besides the space and equipment carrier propagation time delay, also exhibits a group differential phase delay (problem area 3) which results from the passage of the Doppler components through the system. This envelope delay in the RF and video circuitry is negligible. However, the translator and phase detector incorporate narrow bandwidth filters for noise reduction. Large phase errors would result if some means for linearizing the phase versus frequency response of the system were not incorporated. A novel form of translation to the 500-Hz final frequency is used to effect the linearizing process. An equal number of up and down conversions are used with the goal of equating the sum and difference phase delays.

The residual delay is analyzed by the system response to a phase step function. The resultant rise time of 15 msec for the translator and 14 msec for the phase detector, result in an overall rise time of 21 msec. This rise time equates to a frequency response of 17 Hz. For a vehicle traveling at the rate of 1000 m/sec radial velocity, this represents an error in phase of 1.8^{o} or a further error in range of 7.5 m. For the case of the accelerating rocket exhibiting a 50g or 500 m/sec^2 acceleration, this bandwidth represents a cumulative error of 3.8 m/sec^2 during the acceleration time.

The servo system has an adjustable bandwidth up to 10 Hz. Since high acceleration occurs during the launch period at high signal conditions this widest bandwidth is used. The analog record serves to correct high acceleration data when required.

The analog readout device, a Brush MK 280 recorder, has a bandwidth in excess of 60 Hz and, thus, introduces negligible degradation during high dynamic conditions.

In problem area (4), short term statistical variations in tone frequency appear as noise. In general, these are small and are minimized along with system statistical noise by virtue of the very narrow system bandwidth. Any residual can be smoothed in the data reduction process.

The short term drift or an unknown frequency offset can contribute materially to error.

Previously, it was shown that

$$R = \frac{c}{4\pi} \frac{\Delta\phi}{f_I}$$

the error in R as a function of a change in f_I is shown as follows:

$$\frac{\delta R}{\delta f_I} = \frac{c}{4\pi}\left(\frac{f_I \delta\Delta\phi - \Delta\phi}{f_I^2}\right)$$

where $\Delta\phi$ is a measured value and known; therefore, $\delta\Delta\phi = 0$ and

$$\frac{\delta R}{\delta f_I} = -\frac{c}{4\pi}\left(\frac{4\pi f_I \frac{R}{c}}{f_I^2}\right)$$

$$\delta R = -R\frac{\delta f_I}{f_I}$$

This shows that the error is cumulative with range and that the percentage error in range is directly proportional to the percentage error in frequency. The error in measured range incurred by a frequency offset of 1 cycle in the precision range tone at a range of 100 km would be

$$\delta R = \frac{10^5 \text{ meters} \times 1 \text{ Hz}}{10^5 \text{ Hz}} = 1 \text{ meter}$$

Although the tone range system commonly uses an extremely stable, oven-controlled source frequency, very adequate operation can be achieved from a common crystal controlled oscillator.

In problem area (5), the dominant contributions to phase error due to variation in signal level are changes in dynamic loading of tuned circuits as a result of AGC action, variation of conduction angle in mixer circuits, and changes in bias level of ac coupled video circuitry resulting from "Grid Leak" biasing.

Since the tone range system uses standard commercially developed components for the airborne receiver and transmitter plus the ground telemetry receiver, successful operation has been achieved through recognition of the problem accompanied by procurement specifications outlining the maximum acceptable phase deviation over signal dynamic range at a specified carrier deviation. The airborne FM receiver does not use AGC and exhibits extremely good phase stability.

Some insight has been achieved in this area as a result of similar problems encountered in the Radint Interferometer system. AGC variations can be minimized by buffering with follower circuits between a tuned load and the following AGC'd stage. Low Q and broadly tuned loads are used in RF mixer stages.

In the tone translator, filtering, followed by low level limiting and additional filtering, minimizes phase variations resulting from video level change. The use of FM also serves to keep video level constant. Prior to the limiting stage, ac coupled signal processing must be linear class A. Prior to limiting, the video must be referenced to common and direct coupled into the limiter stages. After limiting, the signal is constant, and constant ac coupling will not introduce unknown error.

Closed loop system tests show these variations to be less than 2.2^{o}, which is equivalent to 8 meters for a carrier signal dynamic range of 66 dB, and 2.2^{o}, which is equivalent to 8 meters for a video dynamic level change of 20 dB.

Problem area (6) is in some ways tied to dynamic level errors in that a constant cross-coupled component presents a problem only prior to limiting. After limiting, the cross-coupled component introduces a fixed phase component which can be eliminated. Prior to limiting, the relative resulting phase shift will be a function of the amplitude of the reference tone relative to the cross-coupled component.

The amount of phase offset introduced by cross coupling can be deduced from sketch (c). In this diagram the worst case situation of orthogonality between the undesired component and the desired component is used.

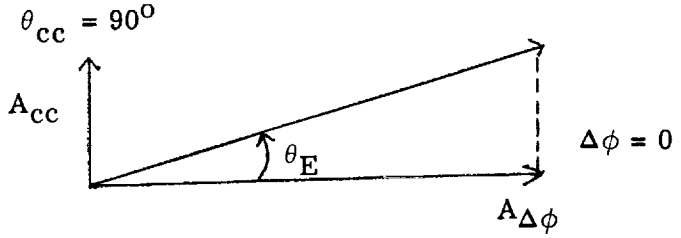

Sketch (c)

where

$\Delta\phi$ range phase difference

$A_{\Delta\phi}$ range phase amplitude

θ_{cc} intermodulation or cross-coupled component phase relative to $\Delta\phi$

A_{cc} coupled phase amplitude

θ_E resulting phase error, $\tan^{-1}\frac{A_{cc}}{A_{\Delta\phi}}$

The following table depicts the range error as a function of relative levels for signal and undesired component:

$\frac{A_{cc}}{A_{\Delta\phi}}$, dB	θ_E, deg	Error, meters, for –		
		Fine tone	Coarse tone	
		100 kHz	2 kHz	4.5 kHz
-10	17.55	73.0	3654	1614
-20	5.72	23.8	1191	526
-30	1.80	7.5	375	166
-40	.57	2.37	119	52
-50	.003	.012	6	3

The results from this table were derived from the following equations. As derived previously

$$R = \frac{c}{4\pi} \frac{\Delta\phi}{f_I}$$

and the resultant range error is

$$(\delta R)_{cc} = \frac{c}{4\pi} \frac{\theta_E \text{ deg}}{f_I} \times \frac{2\pi \text{ rad}}{360 \text{ deg}}$$

$$= \frac{c}{720\, f_I} \theta_E = 4.1639 \times 10^5 \frac{\theta_E}{f_I}$$

Telemetry transmitter intermodulation greater than 1 percent (40-dB voltage) on any IRIG channel is not acceptable for operational use. This criterion is quite sufficient for the tone range introducing a maximum error >3 meters. The intermodulation percentage is, in general, less than that observed on nearby telemetry channels because of the narrower bandwidth of the tone processor. Intermodulation from data channels is, in general, random in nature and any residual can be removed by the data smoothing processes.

The final item, signal to noise, represents a purely statistical distribution of data points centered about the measurement value. The use of narrow band filters in the translator, allows the tracking system to exhibit signal-to-noise characteristics exceeding or identical to those exhibited by the experiment data channels without alloting a large share of the total telemetry transmitter deviation, generally 10 to 20 percent of the total 125-kHz deviation. Under average flight conditions, with the exception of roll induced dropouts, output signal-to-noise conditions are ≧40 dB. This represents a ±1.5 meters

spread which can be reduced to virtually nothing by least squares smoothing. The number of datum samples required to effect adequate accuracy is, of course, an inverse function of the signal-to-noise ratio with the poorest fit occurring during periods of high acceleration. Poor signal-to-noise ratio will, under normal conditions, occur just past apogee and just prior to impact. Fortunately, these are positions of the lowest radial acceleration and thus, materially compensate for any required increase in data smoothing datum points.

In summary, the errors involved are as tabulated in table 1. In the data reduction process, reiterative solutions may be made, incorporating the velocity and acceleration values derived from initial data solution. Tables 2 and 3 indicate the amount of delay error that can be expected in normal flight conditions. Range data from NASA Flight 14.386 GM, a Nike-Apache was processed for velocity and acceleration versus time. The total delay errors were computed under the extreme dynamic conditions shown in table 2 and during a period of general scientific interest, just after apogee, the delay shown in table 2 at $t = 32$ sec decays to 0 at $t = 205$ sec.

Precision and ambiguity.- The precision of a tone range system is a direct function of the highest frequency (Fine) tone. In the previous discussion on accuracy, the frequency of operation has very little impact on the system accuracy, thus, indications are that the Fine Tone may be increased ad infinitum to provide greater and greater precision. There is, of course, the signal-to-noise – bandwidth phase leg trade-off that would indicate an upper limit to the obtainable precision under dynamic conditions. However, these were not the limiting parameters in selection of the Fine ranging tone. Since the requirement for the Tone Range system was based on the need for a redundant means of tracking using the existing FM/FM IRIG telemetry format, the selection of the Fine Range Tone was based on the following considerations:

1. Minimum impact on the telemetry subcarrier format
2. Minimum requirement on telemetry carrier power
3. Use with existing telemetry ground station and airborne equipment (some having bandwidths limited to 100 kHz)

In analyzing the IRIG subcarrier assignments, the notable open frequency slots during the period of initial design were

VCO spectrum	Usable tone	Range ambiguity
Below 370 Hz	None	None
1 828 to 2 127 Hz	2 kHz	75 km
4 193 to 4 995 Hz	4.5 kHz	$33\frac{1}{3}$ km
15 588 to 18 700 Hz	15.8 kHz	9.5 km
Above 80.5 kHz	100 kHz	1.5 km

Rather than take up the space occupied by a data channel, the first system built was designed for a 100-kHz Fine Range Tone and 2 kHz as a Coarse Range ambiguity removing tone. The 75-km ambiguity, although not fulfilling the requirement for range greater than that expected for the vehicle, was sufficient to define position when coordinated with the time into flight and expected vehicle performance. The 2-percent resolution required to remove ambiguity has proved sufficient, although a bit too close to the limit of capabilities under poor signal conditions. The second system built uses a 4.5-kHz $\left(33\frac{1}{3}\text{ km}\right)$ ambiguity removal tone for greater resolution and proves to be a good compromise between resolution under poor signal conditions and selection of an optimal range-length segment for an under- or over-performing vehicle.

With the advent of data channels F, G, and H (upper frequency limit), the 100-kHz tone occupies a position in channel F, just the situation the earlier designs attempted to avoid. The top frequency in this new group is 190 kHz. Future systems will undoubtedly have a choice of 100 kHz or 200 kHz as a Fine tone, although, since future systems must also be capable of working with a PCM-FM telemetry system now being developed, some other frequency may be selected as standard.

The precision of this system at favorable signal to noise and under zero or low dynamic conditions is limited by the resolution of the readout devices. It is a variable under dynamic conditions, being dependent on the amount of improvement made by the reiterative solution process. This has yet to be experimentally determined. However, dynamic errors should be capable of complete elimination since system response under dynamic change is known.

Resolution.- Two readout devices are used to display the range versus time: Brush MK 280 recorder and servo digital readout.

The analog readout device is an 80-mm galvo record subdivided into 50 equal divisions. This record can easily be read to location in 1/3 of a small division or ±5 meters.

The digital readout device is primarily intended for fast computer reduction and is limited in decade capability. It was elected to give this readout an extensive range capability to cover vehicles like the Astrobee 1500 and Javelin rather than greater resolution. The least significant bit represents a change in range of 10 meters.

To summarize, system precision in range equals system resolution; both are analog ±5 meters and digital ±5 meters.

Interferometer Accuracy

From the foregoing system descriptions, one can perceive that the Interferometer suffers identical types of system limitations as those encountered by the Tone Range/TM Interferometer system, inasmuch as the signal processing, measurement technique and display are identical in nature. In fact, since the Radint Interferometer technique had

proven to be very successful at the time of tone range development and the range-phase measurement was recognized to be an identical problem, the Interferometer technique served as a design model for the range processor.

In addition to the system processing errors (those which are covered in the section on tone range accuracy), geometric variations play a dominant role in overall interferometer measurement accuracy. A list of these geometric variations would include such items as

Axis orthogonality and tilt
Axial alinement with respect to geodetic coordinates
Antenna spacing
Antenna element alinement and tilt
Antenna height
Antenna circularity
Antenna cross coupling

Extreme care is taken in the initial layout and installation of the interferometer quadrangle. Geodetic alinement is achieved through observation of the ascension of Polaris (or some other celestial object, if not in the northern hemisphere) and translating by a theodolite to true north. Upon establishing the north-south base leg, the utmost in surveying accuracy is used to establish the other parameters. When completed, the interferometer is essentially "bore sighted" to local zenith. When the antennas are tied into the remainder of the system, extreme care is taken in establishing equal electrical phasing from the antenna through the point of reference phase injection.

For an insight on the procedures used in establishing the interferometer consult reference 5. Preliminary results of an accuracy analysis conducted by James Bassler of the New Mexico State University are presented in table 4. These represent computed standard deviations in position based on range data from a nominal Apache. In this computation of standard deviations, the range values were considered errorless.

Interferometer Precision, Resolution, and Ambiguity

By referring to the "Philosophy of Angle Measurement" section, it can be found that the space angle's θ relationship to electrical phase angle ϕ was

$$\cos\ \theta = \frac{\phi}{2\pi N}$$

where N is the number of wavelengths encompassed by the interferometer base length.

As N increases, the precision in cosine θ also increases; however, survey tolerance buildups and detrimental environment effects impose a definite limit on the base

length. Sixteen wavelengths for the Radint frequency of 73.6 MHz is near the optimum configuration. Due to its higher operating frequency, the Telemetry Interferometer could conceivably be longer and therefore more precise. However at the present time the two systems are tied to each other for convenience and economy. The precision of the interferometer system is tied to its output resolution, this resolution in direction cosine is analog $\pm 5 \times 10^{-5}$ and digital $\pm 5 \times 10^{-5}$. However, interferometer geometry affects this granularity. Earlier, the relationship of the direction cosine to electrical angle was derived as $\cos \theta = \frac{\phi}{2\pi N}$. Differentiating θ with respect to ϕ one obtains

$$\frac{d\theta}{d\phi} = \frac{(1 - \phi^2)^{-1/2}}{2\pi N}$$

When $(1 - \phi^2)^{-1/2}$ is expanded,

$$(1 - \phi^2)^{-1/2} = 1 + \frac{\phi^2}{2} + \frac{3}{8}\phi^4 + \frac{15}{48}\phi^6 + \ldots$$

is obtained. For $\phi = 0^o$, source at zenith, the granularity in θ is equal to the granularity in ϕ. For $\phi = 2\pi N$, source at horizon, the granularity in $\theta \approx \infty$. Table 5 gives the computed space angle granularity for several positions of sounding rocket interest. Lobe ambiguities are depicted in figure 10 with their related data tabulated in table 6. Table 7 summarizes the precision of the Tone Range/TM Interferometer system in comparison with other tracking systems.

OPERATIONAL RESULTS

The Tone Ranging/TM Interferometer system has been in semi-operational status since 1967. During this period, the system has been used to track and produce trajectories for 22 sounding rockets. Fourteen of these rockets were parachute-recoverable payloads. The impact point was calculated for all 14 payloads within 15 minutes of impact. The recovery crews, using the Tone Ranging impact point, recovered the majority of these payloads within 24 hours. Prior to 1967, payload recovery took several months, and one payload was never located.

In an effort to determine the accuracy of this developmental system, comparisons have been made with two other types of tracking systems, radar and Radint. The first comparison shown in table 8 was for Nike-Cajun 10.161 GM launched at Wallops Island in May 1967. The comparison shown is the Wallops Island FPS-16 versus the Tone Range/TM Interferometer system. The table shows a typical altitude comparison every 10 seconds for the first 150 seconds of flight.

The second comparison shown in table 9 was for Nike-Apache 14.333 UM launched in Puerto Rico in March 1968. This comparison is of the Tone Range/TM Interferometer system and Radint. The table shows a typical comparison every 10 seconds for the first 160 seconds.

It is difficult to obtain the absolute accuracy of any tracking system. When making comparisons, the accuracy of the system being used as a standard is always questionable. The systems which were used as a standard for the tone ranging comparisons are accepted by most experts as being quite accurate tracking systems. These comparisons between radar, Radint, and the Tone Range/TM Interferometer system are very promising and show that the Tone Range system is capable of providing an accurate trajectory with an average difference, from the standards used, of plus and minus 30 meters.

CONCLUDING REMARKS

The Tone Range/TM Interferometer system has supported 22 firings and is regarded as prime tracking in support of the Dudley Observatory recoverable payloads at White Sands Missile Range. Although the above situation exists, at the present time, the system is regarded as still being in the prototype development stage.

Results from analysis point out areas for improvement and the overall question of point-of-phase comparison has not had sufficient analysis to unquestionably settle on the translation technique.

Recently, a version of Tone Range, called the Wee Track, has been under evaluation. This system makes direct phase measurement at the 100-kHz level and at present does not incorporate ambiguity removal. Laboratory tests of this system are promising. There are also plans for an early test of a single path system using a highly stable 1×10^{-8} oscillator in the vehicle. It is anticipated that the combination of these latter two experimental devices will provide very economical redundant tracking of any vehicle launched with a telemetry transmitter.

With the advent of S-band operation, the interferometer may evolve into a wide beam X-Y mounted tracking antenna from which coarse angles are derived from the shaft position and corrected from the interferometer phase. This type of operation may be required since higher gain antennas must be used. However, this mode of operation would eliminate the high slew rates required of radar mounts.

Taking note of the desirability of immediate post-flight X-Y-Z position plots, the Sounding Rocket Instrumentation Section is developing an analog computer to provide this capability.

Another development in progress is direct digital conversion circuitry. It is anticipated that this will eliminate some dynamic errors presently found in the servo-system and as a side benefit materially reduce the cost. This method, if successful, will be applied to the interferometer digitization, providing the same benefits.

As it is presently comprised, the system may be installed and operating in the field at costs of from $90 000 to $220 000. The difference in costs relates primarily to whether or not digital capability is included.

REFERENCES

1. Laster, J. A.; Scheibner, J. E.; Anderson, D. P.; Martin, B.; and Silverman, M.: Characteristics and Development Report for the Setrac Model 1. SC-DR-64-525, Vol. II, Sandia Corp., Nov. 1964.

2. Vonbun, F. O.: Analysis of the "Range and Range Rate" Tracking System. NASA TN D-1178, 1962.

3. Kronmiller, G. C., Jr.; and Baghdady, E. J.: The Goddard Range and Range Rate Tracking System: Concept, Design, and Performance. GSFC X-531-65-403, NASA, Oct. 1965.

4. Gill, T. P.: The Doppler Effect. Academic Press, Inc., c.1965.

5. Joosten, W. L.; Sabin, R. J.; Lee, E. D.; Gammill, W. G.; and Montz, W. F.: Manual for the NASA/SSD System. PM00171 (Contract No. NAS 5-3068), New Mexico State Univ., Feb. 1963.

TABLE 1.- SUMMARY OF ERROR CONTRIBUTIONS TO TONE RANGING

Source	Effect	Comments
Dynamic level	12.5 meters	Can be calibrated out from correlation with AGC record
Frequency stability offset	Negligible	Frequency source used is stable 5 parts in 10^{10} per day
Cross-coupling intermodulation	3 meters	40-dB separation in level for both cases
Propagation delay	$(R/3) \times 10^{-8}$ meter per m/sec	Can be all but eliminated by reiterative solutions
Equipment propagation delay	10^{-3} meter per m/sec	Can be all but eliminated by reiterative solutions
Differential phase delay:		
Velocity	75×10^{-3} meter per m/sec	Can be all but eliminated by reiterative solutions
Acceleration	7.6×10^{-3} m/sec per m/sec^2	Can be all but eliminated by reiterative solutions

TABLE 2.- CALCULATED COMBINED RANGE DELAY ERRORS, BOOST AND SUSTAINER PERIODS FOR 14.386 GM

Time, sec	Range, km	Radial velocity, m/sec	Radial acceleration, m/sec^2	Combined position delay errors, meters
0	1.085	0	0	0
1	1.100	76.7	123.5	-1.58
2	1.238	302	327	-5.95
3	1.704	631	332	-11.2
4	2.500	805	17.8	-12.8
5	3.313	795	-37.8	-12.5
6	4.089	755	-43.0	-11.8
7	4.822	712	-43.0	-11.1
8	5.512	672	-36.6	-10.5
9	6.165	636	-34.5	-10.0
10	6.784	604	-29.3	-9.5
11	7.373	576	-26.0	-9.1
12	7.936	551	-25.0	-8.7
13	8.475	527	-21.7	-8.3
14	8.991	507	-19.2	-8.0
15	9.489	487	-21.66	-7.6
16	9.965	467	-19.4	-7.3
17	10.4	451	-16.2	-7.1
18	10.9	434	-17.7	-6.8
19	11.3	417	-15.3	-6.6
20	11.7	405	-8.9	-6.4
21	12.1	396	-26.8	-6.1
22	12.5	394	23.5	-6.3
23	12.9	489	166.5	-8.4
24	13.5	662	178.7	-11.2
25	14.2	852	201.3	-14.33
26	15.2	1071	237.3	-18.0
27	16.3	1334	288.5	-22.5
28	17.8	1577	197.0	-26.1
29	19.5	1670	-9.76	-26.9
30	21.2	1654	-23.2	-26.6
31	22.8	1631	-22.0	-26.2
32	24.5	1610	-19.52	-25.9

TABLE 3.- CALCULATED COMBINED DELAY ERRORS FOR PERIOD NEAR APOGEE 14.386 GM

Time, sec	Range, km	Radial velocity, m/sec	Radial acceleration, m/sec^2	Combined position delay errors, meters
205	156.4	-3.5	-8	0
206	156.4	-11.9	-8	.25
207	156.4	-20.1	-8	.39
208	156.4	-28.4	-8	.54
209	156.3	-36.6	-8	.68
210	156.3	-44.5	-8	.82
211	156.3	-52.6	-8	.97
212	156.2	-60.7	-8	1.11
213	156.1	-68.6	-8	1.25
214	156.1	-76.4	-8	1.39
215	156	-84.2	-8	1.52
216	155.9	-92.3	-8	1.67
217	155.8	-100.5	-8	1.81
218	155.7	-109	-8	1.96
219	155.6	-117	-8	2.10
220	155.5	-124	-8	2.24
221	155.3	-133	-8	2.38
222	155.2	-141	-8	2.52
223	155.0	-148	-8	2.66
224	154.9	-156	-8	2.80

TABLE 4.- STANDARD DEVIATION IN X, Y, AND Z COORDINATES WITH RANGE MEASUREMENT ASSUMED PERFECT. (DATA ARE PRELIMINARY RESULTS FROM A RADINT-INTERFEROMETER-ACCURACY SURVEY MADE WITH FLIGHT MODEL NIKE-APACHE 14.386 GM)

Flight time, sec	Elevation angle, deg	Slant range, km	σ_z, meters	$\sigma_x = \sigma_y$, meters
15	77	10.5	0.7	2.9
30	79	21.2	2.1	10.0
50	79	51.1	4.3	21.4
100	77	109	8.2	36.2
150	75	144	9.4	39.7
200	71	157	13.7	39.7
250	64	149	19.8	40.8
300	51	124	36	44
350	21	98	233	110

TABLE 5.- COMPARATIVE DIRECTION COSINE PRECISION GRANULARITY FOR TM INTERFEROMETER, FPS-16 AND FPQ-6 RADARS

Az, deg	El, deg	Least significant value (parts per 10^5)								
		Radint			FPS-16			FPQ-6		
		X	Y	Z	X	Y	Z	X	Y	Z
0	30	5	5	9	8	5	8	4	2	4
0	50	5	5	4	6	7	6	3	4	3
0	70	5	5	2	3	9	3	2	5	2
0	90	5	5	0	0	10	0	0	5	0
30	30	5	5	12	10	8	8	5	4	4
30	50	5	5	6	9	10	6	5	5	3
30	70	5	5	2	7	10	3	4	5	2
30	90	5	5	4	5	8	0	2	4	0
60	30	5	5	12	8	10	8	4	5	4
60	50	5	5	6	10	9	6	5	5	3
60	70	5	5	2	10	7	3	5	4	2
60	90	5	5	4	8	5	0	4	2	0
90	30	5	5	9	5	8	8	2	4	4
90	50	5	5	4	7	6	6	4	3	3
90	70	5	5	2	9	3	3	5	2	2
90	90	5	5	0	10	0	0	5	0	0

TABLE 6.- DIRECTION COSINES AND SPACE ANGLES FOR HALF OF A 16-λ INTERFEROMETER

Lobe	cos θ	Angle from horizon, θ	Lobe	cos θ	Angle from horizon, θ
16	0.99909	2°27'	7	0.43710	64° 5'
15	.93664	20°30'	6	.37466	68° 0'
14	.87420	29° 3'	5	.31222	71°48'
13	.81176	35°44'	4	.24977	75°32'
12	.74932	41°28'	3	.18733	79°12'
11	.68687	46°37'	2	.12489	82°50'
10	.62443	51°22'	1	.06246	86°25'
9	.56199	55°48'	0	0	90° 0'
8	.49954	60° 2'			

TABLE 7.- RELATIVE DESIGN PRECISIONS FOR SEVERAL TRACKING SYSTEMS

TRACKING METHOD		DESIGN PRECISION	
GENERAL	SPECIFIC	RANGE	AZIMUTH & ELEVATION
DOPPLER INTERFEROMETER SYSTEMS	RADINT	± 1 METER	± .0029 DEGREES
	TONE RANGE-T.M. INTERFEROMETER	± 5 METERS (RESOLUTION LIMITED CASE)	± .0029 DEGREES AVERAGE
RADAR	AN/MPS -19	± 25 YDS = ± 22.8 METERS	± 1 MIL = ± .056 DEGREES
	AN/FPS -16	± 5 YDS = ± 4.58 METERS	± 1 MIL = ± .056 DEGREES
	AN/FPQ -11	± 25 YDS = ± 22.8 METERS	± 0.5 MIL = ± .028 DEGREES
	SPANDAR	± 25 YDS = ± 22.8 METERS	± 1 MIL = ± .056 DEGREES
	AN/FPQ-6	± 5 YDS = ± 4.58 METERS	± 0.05 MIL = ± .0028 DEGREES

TABLE 8.- COMPARISON OF TONE RANGE AND FPS-16 TRACKING SYSTEMS

Time, t, sec	Tone Range - FPS-16, ΔZ, meters	Altitude, Z, meters
10	-17.1	5 720
20	-36.6	12 140
30	-38.4	22 620
40	-36.6	31 956
50	-35.3	41 983
60	-35.3	47 013
70	-37.5	53 251
80	-39.6	58 364
90	-40.5	62 650
100	11.3	65 720
110	10.6	68 250
120	-33.5	69 495
130	-39.5	69 750
140	-26.2	69 400
150	-35.8	67 600

TABLE 9.- COMPARISON OF TONE RANGE AND RADINT TRACKING SYSTEMS

Time, t, sec	Tone Range - Radint, ΔZ, meters	Altitude, Z, meters
10	3.9	6 678
20	4.2	11 414
30	19.2	21 756
40	-4.2	37 078
50	-6.1	51 170
60	-3.0	64 250
70	-8.5	76 385
80	-18.5	87 555
90	-21.5	97 767
100	-25.3	107 027
110	-34.8	115 347
120	-40.5	122 713
130	-46.0	129 128
140	-51.5	134 606
150	-44.2	139 140
160	-33.5	143 956

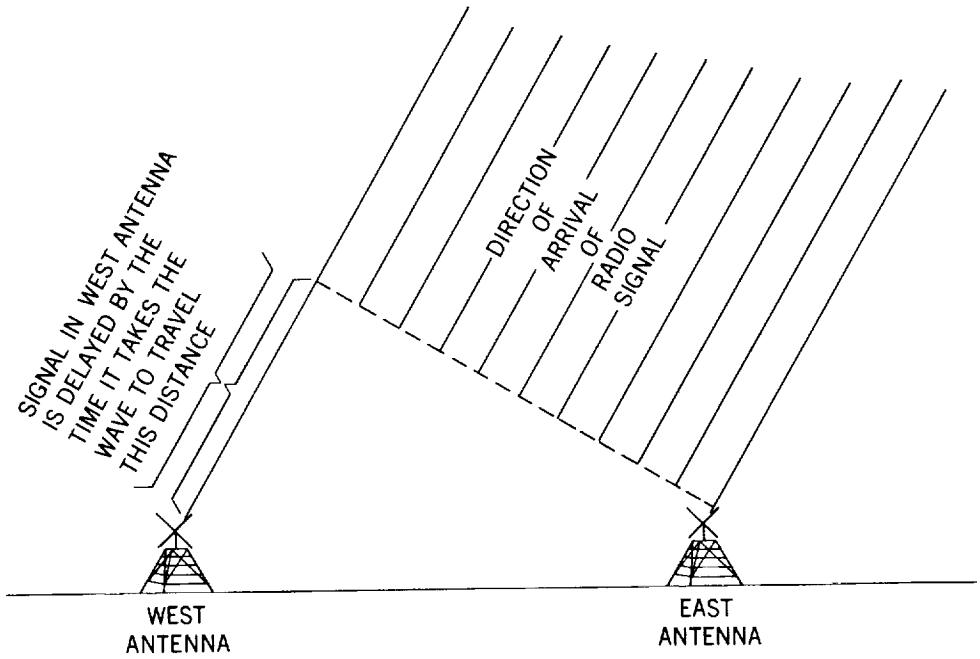

Figure 1.- Interferometer geometry.

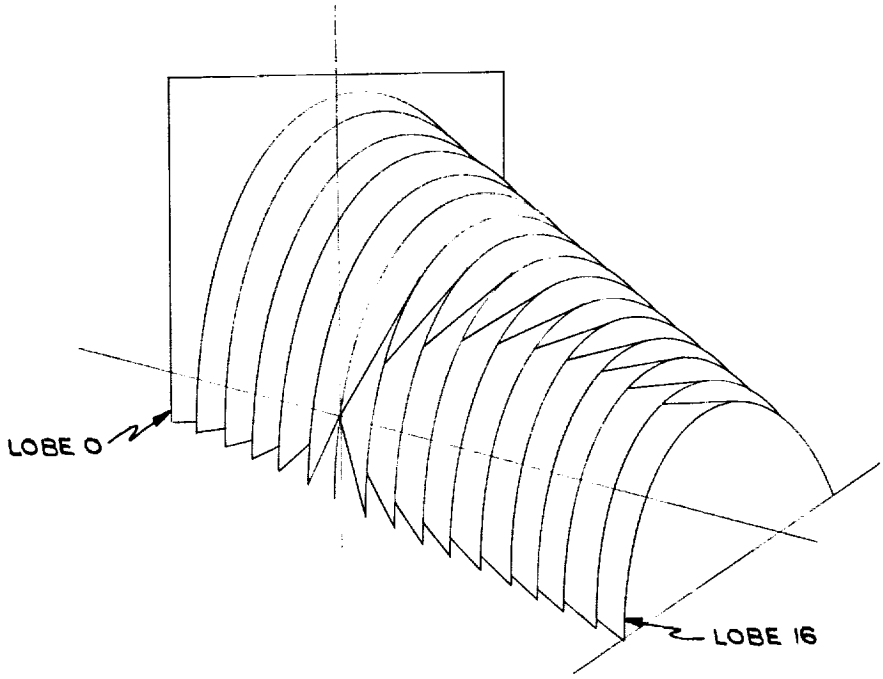

Figure 2.- Spacial distribution of interferometer lobes. (Lobes extend to infinity.)

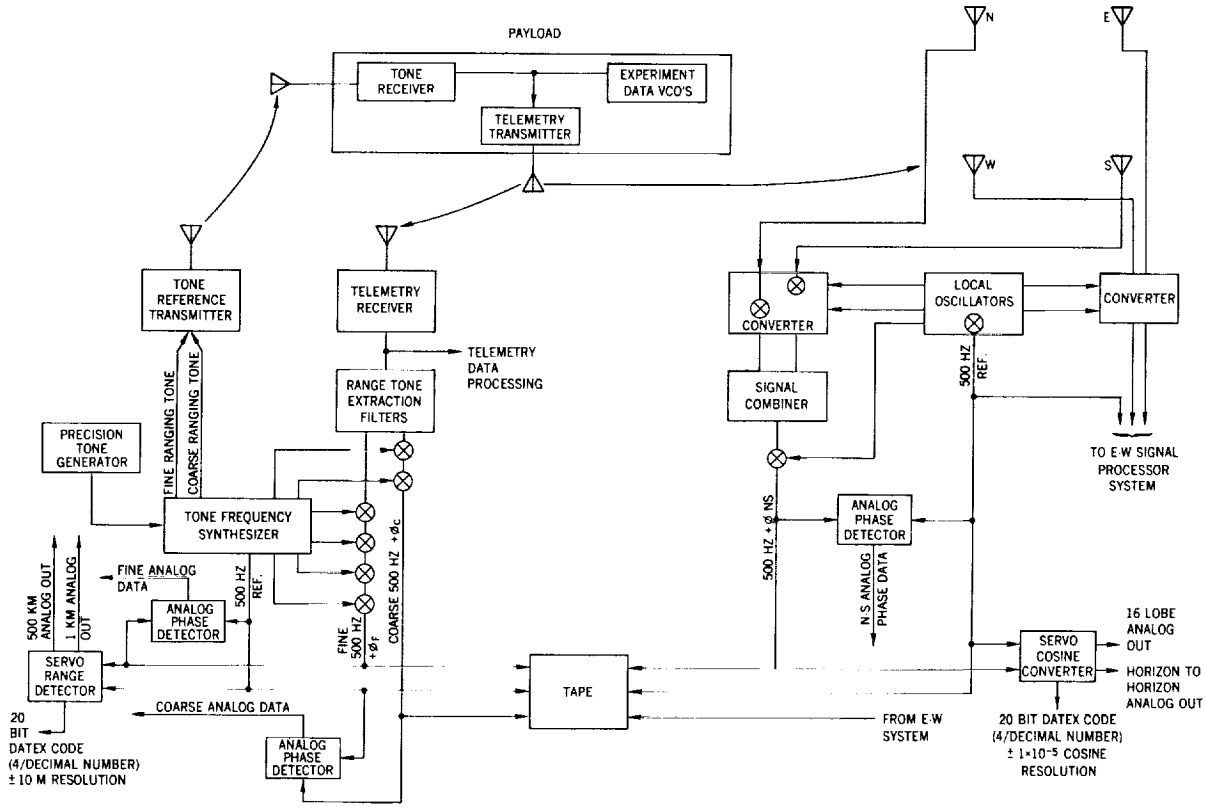

Figure 3.- Tone Range/Telemetry Interferometer systems.

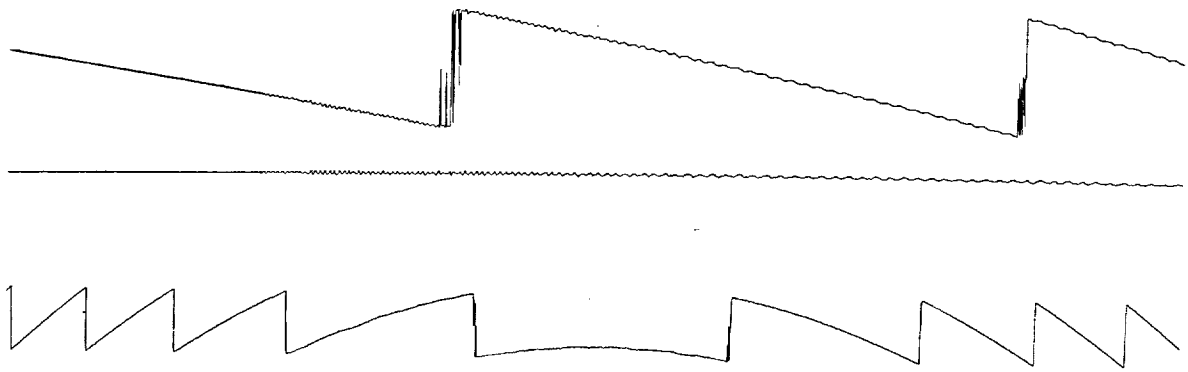

Figure 4.- Segment of a typical range analog record.

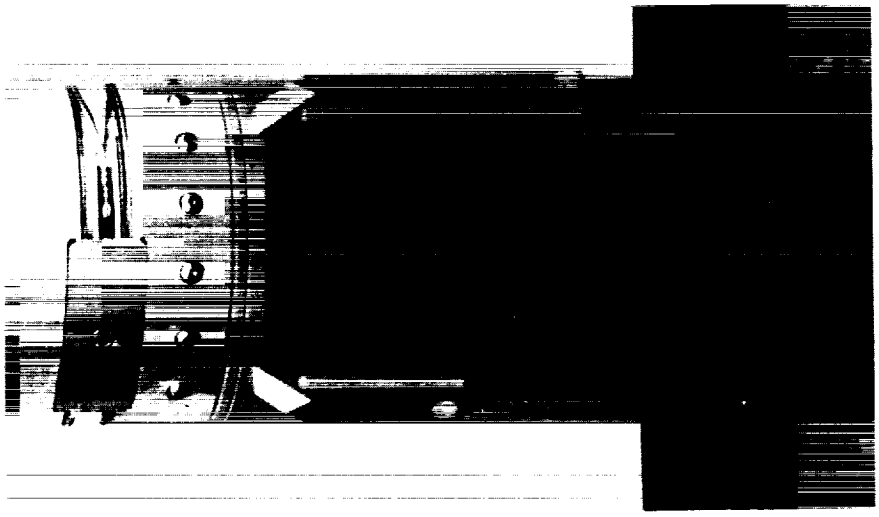

Figure 6.- Telemetry and range receiver antennas mounted on payload.

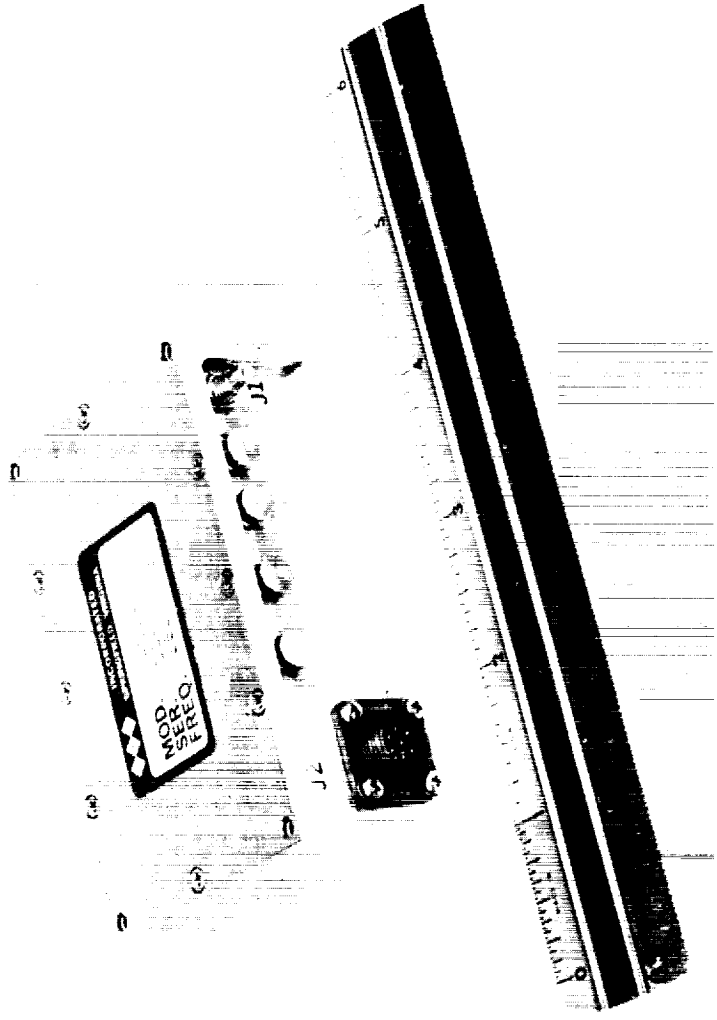

Figure 5.- Airborne range tone receiver.

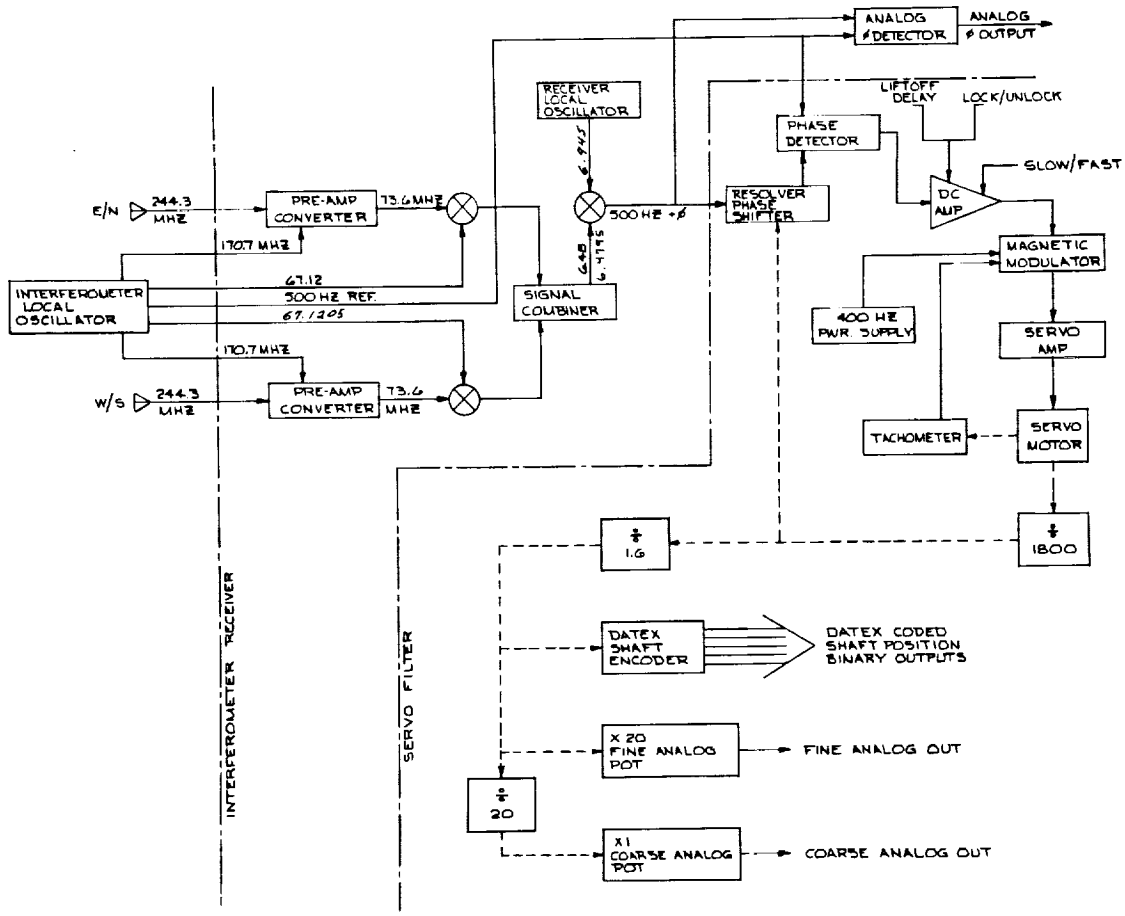

Figure 7.- Interferometer system, simplified block diagram.

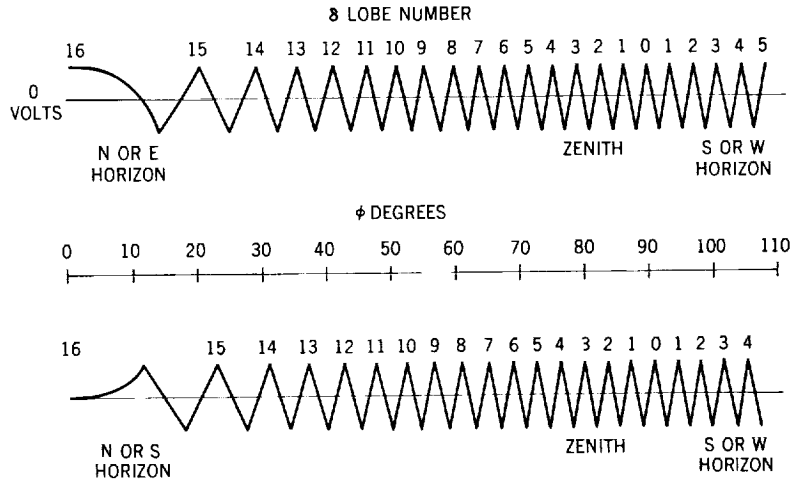

Figure 8.- Continuous analog output of interferometer phase detector.

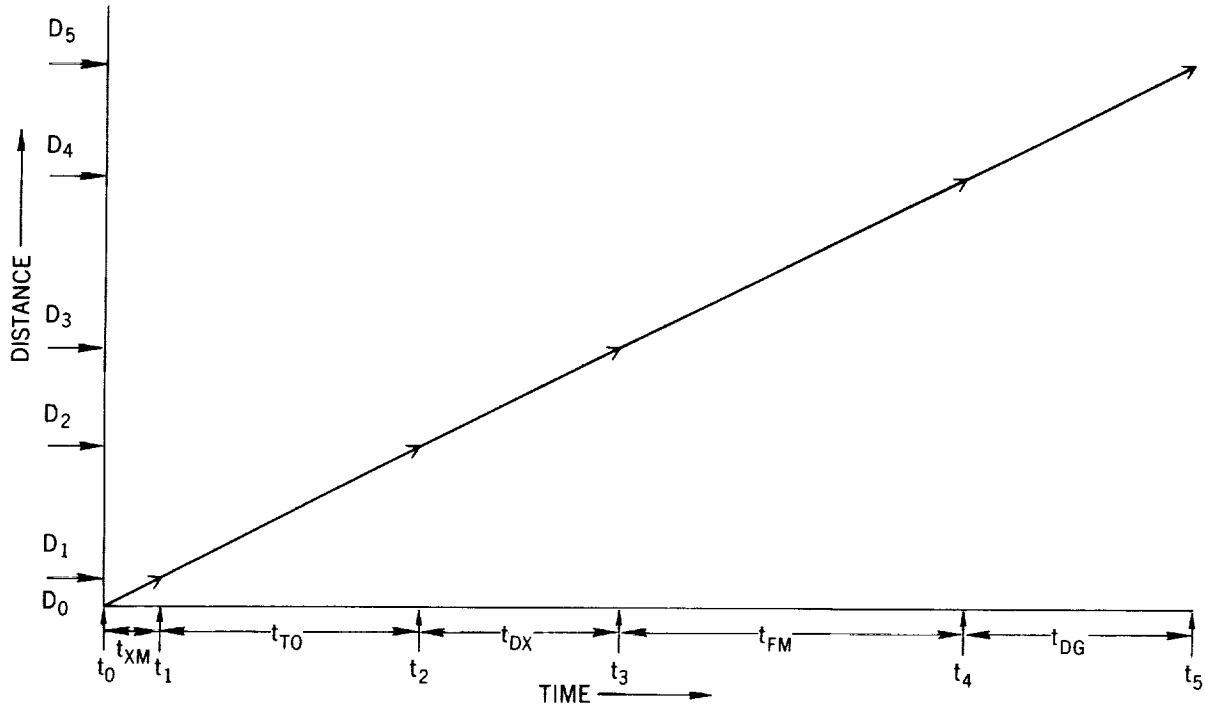

Figure 9.- Impact on measurement accuracy by group delays for a constant velocity.

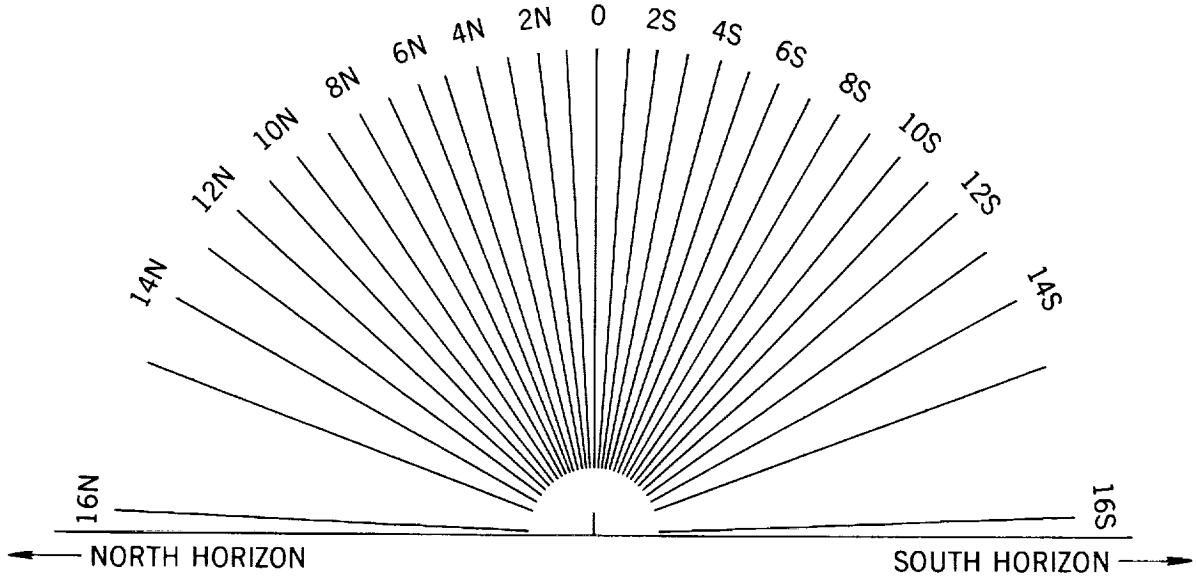

Figure 10.- Slant plane lobe diagram. North-south array.